A QUICK DESIGN TOOL FOR DCB BONDED JOINTS BASED ON A COHESIVE ZONE MODEL AND AN ANALYTICAL ELASTIC FOUNDATION MODEL

Albert Turon[2], Mario Cabello[1], Carlos Sarrado[2], Javier Zurbitu[1], Jordi Renart[2], Félix Martínez[1]

[1]IK4-IKERLAN Technology Research Centre, Pº.J.Mª. Arizmendiarrieta 2, Mondragn, Spain
Email: mjcabello@ikerlan.es, Web Page: http://www.ikerlan.es
[2]AMADE, Polytechnic School, University of Girona, Campus Montilivi s/n, 17071 Girona, Spain
Email: albert.turon@udg.edu, Web Page: http://www.udg.edu

Keywords: DCB test, adhesive joints, composite, cohesive laws, J-integral, analytical model

Abstract
The simulation of the nonlinear mechanical behaviour of bonded joints requires the definition of very fine meshes and non-linear material models that may increase a lot the computational time and effort needed for the prediction of the failure loads. Therefore, the incorporation of advanced numerical simulation tools in the design process is usually not possible. For these reasons, it is of high interest the development of quick design tools, based for example on analytical models, with a very low computational effort and with a reasonable accuracy for the prediction of the mechanical behaviour of bonded joints. In this work, this point is addressed for DCB bonded joints with flexible and stiff adhesives and/or thick and thin adhesive layers. An analytical model based on beam theory, an elastic Winkler foundation model and combined with a progressive damage model based on the cohesive zone approach is presented. The general elastic foundation model recently developed by the authors [1] has been enhanced with a cohesive zone model formulation for the prediction of the mechanical behaviour of adhesive joints [2]. The model is implemented in Matlab and can predict the whole load- displacement curve of a DCB specimen in few seconds. Moerover, their capability to accurately predict the failure load of DCB bonded joints and other joint configurations is demonstrated. A comparison of the prediction of the model with a finite element simulation using cohesive elements also demonstrates the reliability of the model and the comparison on the computational time, highlights the benefits of the presented model.

1. Introduction

The increase of new materials in modern industry is a challenge for joint processes on assembled parts. Different techniques are used with this purpose but in recent years adhesively bonded joints have been of special interest due to the advantages when different materials are bonded together [1]. In the last decades, numerous analysis methods have been specially developed for the design of adhesive bonded joints, nevertheless there is not still a general model valid for any kind of adhesive. Advanced computational techniques, such as the finite element method (FEM), are becoming the principal tools used for designing adhesive joints, however analytical models remain of interest to designers due to their ability to provide fast calculations.

There are different analytical models to predict the elastic behaviour and failure of adhesive joints [2, 3]. These models generally make assumptions and are limited to certain loading conditions and failure modes. Under mode I loading, the double cantilever beam (DCB) test is a common setup to study

Excerpt from ISBN 978-3-00-053387-7

the failure process on adhesive bonded joints. The simplest DCB analytical model is based on simple beam theory, assuming a clamped condition at the crack front of the specimen and crack growth is predicted based on linear elastic fracture mechanics (LEFM) approaches, i.e., when the energy release rate available at the crack tip reaches the fracture toughness of the adhesive. However, this approach is limited to very stiff adhesives and thin adhesive layers, and does not describe the true deflection of the specimen arms near the crack front. In order to improve the estimation of the stiffness, correction factors have been incorporated to the formulation [4] (Corrected Beam Theory data reduction method). But these approaches are limited to very thin adhesive layers, whose elastic contribution is dismissed in the formulation.

Additionally, enhanced DCB models have been proposed in the literature incorporating interface elasticity into the model using Winkler elastic foundation beam theory [5–9]. With these models the energy release rate is obtained as a function of an equivalent crack and the apparent Young's modulus of the adhesive. To obtain the apparent Young's modulus different approaches are considered. One that has enjoyed great success is the work of Jumel et al. [7] for thin adhesive layers, which assumes a transversal plane strain condition for the adhesive. However, the model has some limitations such as it is only applicable in cases when the thickness of the adhesive is small to and the material is compressible. To solve these limitations, a general model was recently proposed by the authors [10]. Cabello's model uses an empirical correction of the stress distribution on the adhesive layer. The apparent Young's modulus of the adhesive is a function of the transverse position in the adhesive midplane. Using this correction, the stress distribution assumed within the adhesive layer is more accurate. The model predicts the elastic behaviour of the adhesive layer but it does not include any mechanism to simulate the crack propagation. To predict bond failure due to crack propagation, analysis models based on the Cohesive Zone Models (CZM) can be used. CZMs are able to accurately reproduce the fracture process zone (FPZ) that develops ahead of a crack tip and, therefore, accurately simulate the load redistribution due to damage and the progressive failure of adhesive joints. Cohesive zone models are usually developed in a finite element framework [11–15]. They are actually the most common numerical method to predict the adhesively interface separation, however fine meshes and higher computational cost are required to obtain accurate results. Different cohesive laws have been proposed in the literature, but normally assumptions of zero adhesive thickness are made. Recently, Sarrado et al. [16] presented a finite cohesive element with thickness to capture the influence of the adhesive elasticity on the damage development. The aim of the present paper is to propose a new analytical model with coupled progressive cohesive damage to predict failure process of an adhesive joint loaded under mode I. The model is based on Euler beam on Winkler elastic foundation theories. The foundation stiffness accounts for the elasticity of the adhesive layer and is coupled with a cohesive zone model (Fig. 1).

The model is used for the analysis of bonded joints with two different adhesives (flexible and stiff). The progressive failure of the DCB specimen predicted by the proposed model has been compared to different experimental results and finite element simulations.

2. Analytical model based on beam on elastic foundation coupled with cohesive damage

2.1. General analytical DCB model based on beam on elastic foundation

The general model presented by the authors [17] in a recent publication is used as the basis of the formulation of the coupled model. The general DCB model is based on beam on elastic foundation and it is defined using beam theory assumptions and modelling the behaviour of the adhesive layer using an infinite set of springs with stiffness k. The initial length of the springs is equal to the thickness of the adhesive layer and their deformation defines the magnitude of an equivalent distributed load q; view more details in [5, 17]. The distributed load of the foundation is obtained by integrating the stresses

Excerpt from ISBN 978-3-00-053387-7

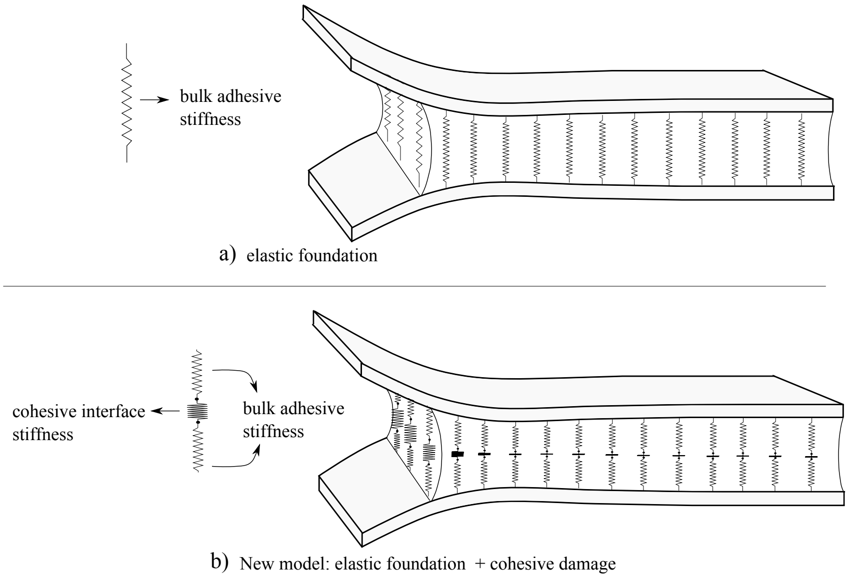

Figure 1. Comparison between a DCB model based on elastic foundation beam theory a) without a progressive damage b) coupled with a cohesive zone model.

along the specimen width [10], and the stiffness foundation is:

$$k_y = E_a^{\prime(eq)} B_t^* \tag{1}$$

where E_a is the apparent Young's modulus of the adhesive layer and B_t^* a geometric parameter. Both parameters depend on the stress stated considered for the analysis. A summary of different approaches used in the literature to simulate is shown in Table 1.

Stiffness foundation $k_y = E_a^{\prime(eq)} B_t^*$	Cabello et al. [10] (general model)	Jumel [7] $(\{x, B\} \gg t_a)$	Krenk [5] $(\{x, B\} \ll t_a)$
$E_a^{\prime(eq)}$	$\frac{(1-\nu_a)E_a}{(1+\nu_a)(1-2\nu_a)+\psi_x}$	$\frac{(1-\nu_a)\,E_a}{(1+\nu_a)(1-2\nu_a)}$	E_a
B_t^*	$\frac{B}{t_a} - \ln\left(\frac{1-\nu_a-\nu_a^2+\psi_x}{(1+\nu_a)(1-2\nu_a)+\psi_x+\psi_{(B/2)}}\right)^{6\nu_a}$	B/t_a	

Table 1. Stiffness of the elastic foundation from different authors. E_a, ν_a are the adhesive Young modulus and Poison's ratio, and t_a is the thickness of the adhesive layer. B is the width of the specimen.

The general model proposed in [10] includes the other approaches of the literature as a particular cases, e.g. if the distance to crack front x and the width of the specimen B are larger than the adhesive thickness t_a, the correction functions become $\psi_x = 0$ and $\psi_{(B/2)} = 0$ and the stiffness foundation of the general model match with Jumel's model [7]; on the contrary, if x and B tend to zero (at the edges of the adhesive layer), the correction functions become $\psi_x = \psi_{(B/2)} = \nu_a^2$ and the stiffness foundation of the model matches with the solution proposed by Krenk [5].

Excerpt from ISBN 978-3-00-053387-7

2.2. Stiffness foundation model coupled with a progressive damage model

The models presented in previous section assume a linear elastic behaviour of the adhesive layer. This approach is valid at early stages of the deformation process, but if the adhesive layer is highly loaded, inelastic processes develop and the equivalent stiffness of the foundation is not longer constant. A cohesive zone model coupled with the stiffness foundation model is used in this work to describe the degradation process prior to cohesive failure of the adhesive layer. A similar approach as proposed in Sarrado et al. [16] is used to couple both models. In [16] the model was implemented in a finite element code using a cohesive element with a finite thickness, in the present paper, an analytical solution is provided. The model assumes that the elastic and nonlinear deformation can be modelled with two sets of springs working in series. Therefore, the deformation of the adhesive layer is divided into two terms: the elastic elongation of the adhesive layer $\delta_y^{(adh)}$ and the nonlinear elongation due to damage $\delta_n^{(coh)}$.

The nonlinear processes are collapsed to a surface located at the midplane of the adhesive layer, and these nonlinear processes are modelled using a bilinear cohesive law, based on the model of Turon et al. [14]. The relation between the cohesive traction τ_n and the nonlinear elongation (cohesive displacement jump) $\delta_n^{(coh)}$ reads

$$\tau_n = \frac{\tau_n^{max}}{\delta_n^{(o)}}(1 - D_n)\delta_n^{(coh)} \tag{2}$$

where τ_n^{max} is the maximum cohesive traction and $\delta_n^{(o)}$ the normal cohesive displacement jump corresponding to the maximum normal traction. Using a bilinear cohesive law and the elastic foundation model proposed by Cabello et al. [10], the equivalent stiffness foundation, equation (1), is now updated incorporating the damage parameter and redefining the geometric term $B_t^{*(eq)}$ as a function of the applied displacement:

$$k_y = E_a'^{(eq)}(1 - D_{k_y})B_t^{*(eq)} \tag{3}$$

where the damage on elastic foundation D_{k_y} is now function of an equivalent $E_a'^{(eq)}(x)$ Young's modulus reads,

$$D_{k_y} = \begin{cases} 0 & : (2u_y) \leqslant \tau_n^{max} t_a / E_a'^{(eq)} \\[2ex] \dfrac{2E_a'^{(eq)}/(\tau_n^{max} t_a) - 1/u_y}{2E_a'^{(eq)}/(\tau_n^{max} t_a) - \tau_n^{max}/J_{Ic}} & : \tau_n^{max} t_a / E_a'^{(eq)} < (2u_y) < 2J_{Ic}/\tau_n^{max} \\[2ex] 1 & : (2u_y) \geqslant 2J_{Ic}/\tau_n^{max} \end{cases} \tag{4}$$

and the equivalent width to thickness ratio $B_t^{*(eq)}$ is

Excerpt from ISBN 978-3-00-053387-7

$$
B_t^{*(eq)} = \begin{cases} \text{Eq.}\dfrac{B}{t_a} - \ln\left(\dfrac{1-\nu_a-\nu_a^2+\psi_x}{(1+\nu_a)(1-2\nu_a)+\psi_x+\psi_{(B/2)}}\right)^{6\nu_a} & : (2u_y) \leqslant \tau_n^{max} t_a / E_a'^{(eq)} \\ \dfrac{B}{t_a} - \ln\left(\dfrac{1+\dfrac{{\nu_a}^2}{(1+\nu_a)(1-2\nu_a)+\psi_x} - \dfrac{2\,E_a'^{(eq)} J_{Ic}}{t_a(\tau_n^{max})^2}}{1+\dfrac{\psi_{B/2}}{(1+\nu_a)(1-2\nu_a)+\psi_x} - \dfrac{2\,E_a'^{(eq)} J_{Ic}}{t_a(\tau_n^{max})^2}}\right)^{6\nu_a} & : \tau_n^{max} t_a / E_a'^{(eq)} < (2u_y) < 2J_{Ic}/\tau_n^{max} \\ -\text{undefined}- & : (2u_y) \geqslant 2J_{Ic}/\tau_n^{max} \end{cases} \quad (5)
$$

3. Model validation and discussion of results

3.1. Validation methodology

An experimental campaign of DCB tests was carried out with two different adhesives. The experimental tests were simulated using the analytical model proposed and numerical simulation with finite elements. The results of the analytical models have been compared with the FEM results and the experimental data.

3.1.1. Experimental DCB tests

Two different adhesives are used, one flexible (Silkron-H100) and another stiff (Araldite-2021). All specimens used in this work were cured in a climatic chamber. All DCB tests were performed in a MTS-Insight testing machine at room temperature. The mechanical properties needed for the proposed model are the fracture energy, the elastic properties and the ultimate strength of the adhesive. The elastic properties and ultimate strength are take taken from tensile tests given in [10] and summarized in Table 2 for both adhesives.

Property	Araldite-2021	Silkron-H100
Young's modulus (MPa)	1590	4
Poisson's ratio (-)	0.35	0.4996
Ultimate strength (MPa)	22.6	2.2

Table 2. Adhesive properties determined experimentally from the tensile test using standards ISO-37 [18] and ASTM-D638 [**?**].

The fracture energy was obtained by means of an experimental campaign of DCB tests. Two batches of 20 specimens were tested for both adhesive types using the setup recommended in ISO-25217 [18]. The DCB specimens consisted of two metallic adherends bonded by an adhesive layer. The adherends were 2-mm-thick calibrated steel hand-rails type AISI-420 with a yield strength of 650 MPa, Young's modulus E_s = 200 GPa and Poisson's ratio $\nu_s = 0.33$. The initial crack used was a_0 = 20 mm and specimen length L = 180 mm. The width of the specimens were B = 25 mm and the thickness t_a = 1 mm and t_a = 2 mm for stiff and flexible adhesives, respectively. The tests were performed using a universal testing machine with a crosshead rate of 2 mm/min controlled by displacement and using a video camera to monitor the crack tip position. Two inclinometers, at point of load application, were also used to compute the J-integral. The value of the fracture energy, used for the analytical and numerical models are taken as the mean value in the self-similar crack growth regime, i.e., J_{Ic} = 1.56 N/mm for the Stiff Araldite-2021 adhesive and for 5.48 N/mm for the flexible Silkron-H100 adhesive.

Excerpt from ISBN 978-3-00-053387-7

3.1.2. 3D finite element model simulation using cohesive elements

The DCB tests, for the two adhesive joints, were simulated by means of 3D Finite Element Models in ANSYS [19]. The adherends were modelled using SOLID185 8-node quadrilateral elements with their respective linear elastic material properties. The adhesive layer was modelled using SOLID185 8-node quadrilateral elements with the elastic material properties of the adhesive given in Table 2 and a row of cohesive interface elements (INTER205) at the midplane of the adhesive layer. The cohesive law was assumed bilinear with a very low penalty stiffness in accordance with the linear law implemented in the analytical model. The interface strengths of the adhesives are listed in Table 2 and their fracture toughnesses obtained from the J-integral reported in previous section. The mesh was constructed taking advantage of the automatic meshing algorithms of ANSYS and manual resizing obtaining an element size of 0.25 mm. The loading device was simulated by a combination of rigid beams that reproduce the experimental setup. The mesh and boundary conditions of the model used in the simulations are sketched in Fig. 2.

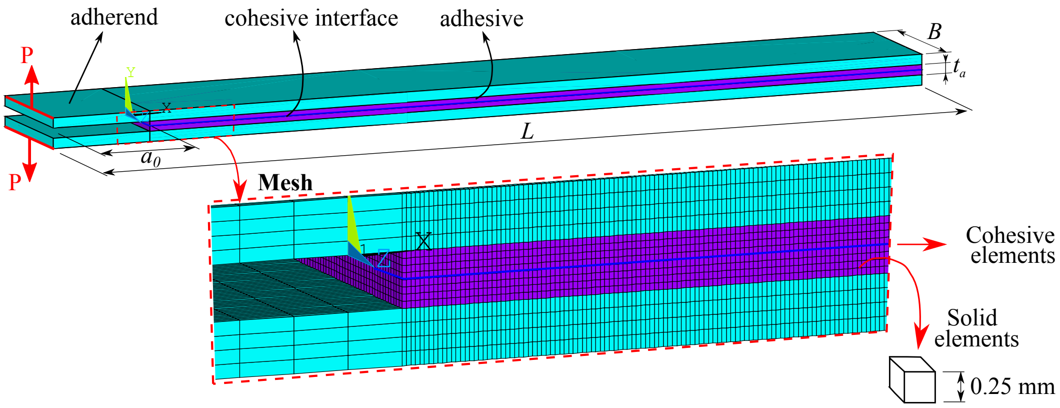

Figure 2. Mesh and boundary conditions used in finite element DCB model.

3.2. Load-displacement curve predicted by the model

The load-displacement curves obtained from the experimental tests are compared with the predictions of the analytical model implemented in Matlab. For the stiff adhesive (Fig. 3a) all models provide similar results, and they are in close agreement with the experimental data. In the self-similar crack propagation regime the predictions of all models fall between the envelope of the experimental data. However, the peak load is underpredicted in all cases, but this is attributed to the fracture toughness used in the models. For flexible adhesives (Fig. 3b) the behaviour is completely different. There is a large non-linear region where damage develops decreasing the apparent stiffness. A very good correlation between experimental tests and the analytical model is obtained. Therefore, for both adhesive types, the results of the FEM simulation are very similar to those obtained with the coupled analytical models, but the computation time is significantly higher.

4. Conclusions

A new analytical DCB model has been proposed based on elastic foundation beam theory coupled with a cohesive zone damage model using a bilinear cohesive law. The model captures the influence of the stress-strain state and the influence of the width to thickness ratio on the equivalent stiffness foundation of the adhesive layer. The model can also be applied to fully incompressible materials.

Excerpt from ISBN 978-3-00-053387-7

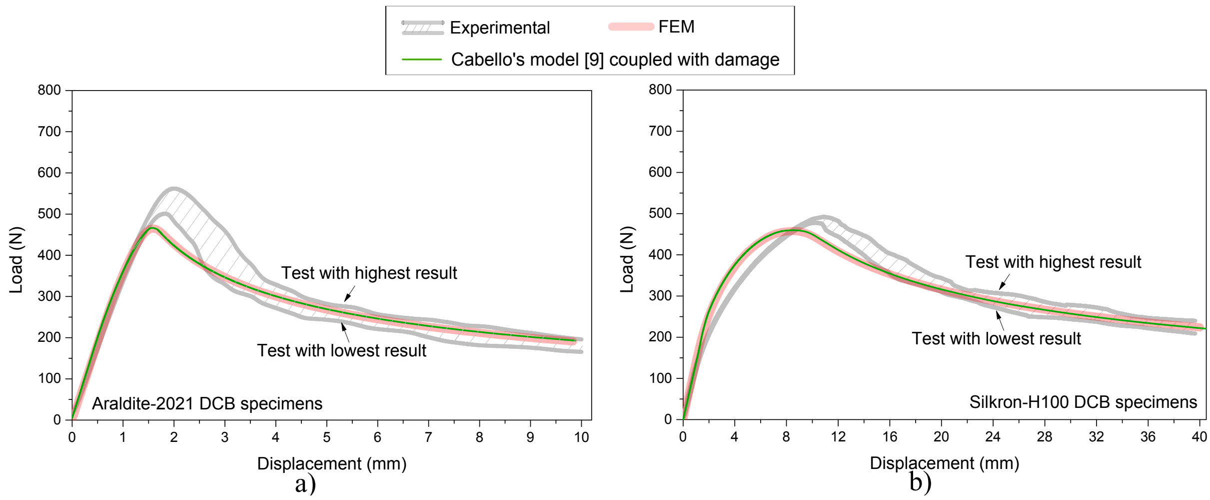

Figure 3. Load-displacement curve obtained by different models in comparison with experimental DCB test for a) Araldite-2021 and b) Silkron-H100 specimens.

The model has been implemented in Matlab. The computational time is very low compared to the comutational time of 3D finite element simulations. The model proposed has been validated against DCB experimental tests with steel adherends and both flexible Silkron-H100 and stiff Araldite-2021 adhesives. A good correlation between the experimental results and the model coupled with cohesive damage has been observed for both types of adhesives in terms of damage process, adhesive stresses at the midplane of the adhesive layer, and load-displacement curve predictions.

Acknowledgments

The authors gratefully acknowledge the financial support of the Spanish government through DGICYT under Contract No. TRA2015-71491-R.

References

[1] Hartmut Pasternak and Yvonne Ciupack. Development of Eurocode-based design rules for adhesive bonded joints. *International Journal of Adhesion and Adhesives*, 53:97–106, sep 2014.

[2] Lucas F.M. da Silva, Paulo J.C. das Neves, R.D. Adams, and J.K. Spelt. Analytical models of adhesively bonded jointsPart I: Literature survey. *International Journal of Adhesion and Adhesives*, 29(3):319–330, apr 2009.

[3] René Quispe Rodríguez, William Portilho de Paiva, Paulo Sollero, Marcelo Ricardo Bertoni Rodrigues, and Éder Lima de Albuquerque. Failure criteria for adhesively bonded joints. *International Journal of Adhesion and Adhesives*, 37:26–36, sep 2012.

[4] B. Blackman, J. P. Dear, A. J. Kinloch, and S. Osiyemi. The calculation of adhesive fracture energies from double-cantilever beam test specimens. *Journal of Materials Science Letters*, 10(5):253–256, 1991.

[5] Steen Krenk. Energy release rate of symmetric adhesive joints. *Engineering Fracture Mechanics*, 43(4):549–559, 1992.

Excerpt from ISBN 978-3-00-053387-7

[6] Jialai Wang and Chao Zhang. Three-parameter, elastic foundation model for analysis of adhesively bonded joints. *International Journal of Adhesion and Adhesives*, 29(5):495–502, July 2009.

[7] Julien Jumel, Michal K. Budzik, and Martin E.R. Shanahan. Beam on elastic foundation with anticlastic curvature: Application to analysis of mode I fracture tests. *Engineering Fracture Mechanics*, 78(18):3253–3269, December 2011.

[8] M.K. Budzik, J. Jumel, and M.E.R. Shanahan. On the crack front curvature in bonded joints. *Theoretical and Applied Fracture Mechanics*, 59(1):8–20, June 2012.

[9] A B De Morais. Mode I cohesive zone model for delamination in composite beams. *Engineering Fracture Mechanics*, 109:236–245, 2013.

[10] M. Cabello, J. Zurbitu, J. Renart, A. Turon, and F. Martínez. A general analytical model based on elastic foundation beam theory for adhesively bonded DCB joints either with flexible or rigid adhesives. *Submitted to: International Journal of Solids and Structures*, pages –, 2016.

[11] C Su, Y.J Wei, and L Anand. An elasticplastic interface constitutive model: application to adhesive joints. *International Journal of Plasticity*, 20(12):2063–2081, dec 2004.

[12] Bent F Sørensen. Cohesive law and notch sensitivity of adhesive joints. *Acta Materialia*, 50:1053–1061, 2002.

[13] Peter Schmidt and Ulf Edlund. Analysis of adhesively bonded joints: a finite element method and a material model with damage. *International Journal for Numerical Methods in Engineering*, 66(8):1271–1308, may 2006.

[14] A. Turon, P. P. Camanho, J. Costa, and C. G. Dávila. A damage model for the simulation of delamination in advanced composites under variable-mode loading. *Mechanics of Materials*, 38(11):1072–1089, 2006.

[15] Xiaocong He. A review of finite element analysis of adhesively bonded joints. *International Journal of Adhesion and Adhesives*, 31(4):248–264, jun 2011.

[16] Carlos Sarrado, Frank A. Leone, and Albert Turon. Finite-thickness cohesive elements for modeling thick adhesives. *Engineering Fracture Mechanics*, mar 2016.

[17] M. Cabello, J. Zurbitu, J. Renart, A. Turon, and F. Martínez. A non-linear hyperelastic foundation beam theory model for double cantilever beam tests with thick flexible adhesive. *International Journal of Solids and Structures*, 80:19–27, 2016.

[18] ISO. ISO-25217 Determination of the mode 1 adhesive fracture energy of structural adhesive joints using double cantilever beam and tapered double cantilever beam specimens. Technical report, International Organization for Standardization, 2009.

[19] ANSYS-Inc. Ansys mechanical, release 15.0, 2014.

Excerpt from ISBN 978-3-00-053387-7